






Low-energy band structures in light odd- A La isotopes using the quasiparticle-phonon coupling plus rotor approach

Z. Housni ¹, A. Khouaja,^{1,*} J. Inchaouh,¹ M. L. Bouhssa ^{1,2}, M. Mouadil,¹ N. Harakat ^{1,2},
M. Fiak ¹ and Y. Elabssaoui ¹

¹Department of Physics, LPMC-ERSA, Faculty of Sciences Ben M'Sik, Hassan II University, Casablanca, Morocco

²Laboratory LPNAMME, GPTN Group, Department of Physics, Faculty of Sciences, Chouaïb Doukkali University, El Jadida, Morocco



(Received 16 December 2020; accepted 9 March 2021; published 8 April 2021)

Quasiparticle-phonon coupling based on one quadrupole phonon is investigated to study the low-energy states of the $A \approx 130$ mass transitional region. The coupling is constructed by using the deformed average field of Nilsson, monopole pairing interaction, and quadrupole-quadrupole forces. Microscopic structure of the quadrupole phonon is given from the Tamm-Dancoff approximation. The effects of the recoil and Coriolis forces are included with the assumption of axially symmetric rotational motion. Since theoretical treatment is performed for odd- A nuclei, the configuration of intrinsic states contains both one-quasiparticle and quasiparticle-phonon components. This model is applied to describe the systematic structure of ^{121}Cs , ^{125}Pr , and $^{123,125,127,129}\text{La}$ nuclei, showing a reasonable agreement with the available experimental data at low excitation energies. From isotonic systematics, a strong Coriolis effect is revealed for negative-parity states and a strong pairing effect is shown for positive-parity ones. For the first time, the lowest (ground) $5/2^+$ state of ^{123}La is proposed to belong to the $1/2^+[420]$ band from the isotopic systematic trend.

DOI: [10.1103/PhysRevC.103.044310](https://doi.org/10.1103/PhysRevC.103.044310)

I. INTRODUCTION

We studied the low-energy quasiparticle structure of odd-mass lanthanum isotopes of the transitional region situated in $55 \leq Z \leq 59$ and $64 \leq N \leq 72$. Several experimental investigations, using β/EC (electron capture) decay, have been carried out to study the low-energy collective states for a variety of neutron-deficient nuclei from this region [1–18]. The experimental observations evidenced both collective and intrinsic excitations in odd-mass nuclei and other structure features such as shape coexistence, γ -vibrational, states and different rotational structure bands [17–28]. The resulting level schemes appeared, however, to be more complicated than those of spherical or deformed nuclei, which make them an ideal testing ground for various theoretical models.

One of the most popular models is the particle plus triaxial rotor model (PTRM) [29,30]. It was first used to give qualitative interpretation of high-spin states in $^{129,131}\text{Ce}$ [23], ^{129}Ba [24], and ^{125}Ba [25]. Another model used in the study of odd-mass nuclei is the interacting boson-fermion model (IBFM) [31]. As an example, it provided a good description in the transitional region, particularly for $^{125,127}\text{Xe}$ [32]. Both models perfectly exhibited the $\pi h_{11/2}$ orbital driving effect and supported earlier predictions of an oblate-prolate shape transition in the $A \approx 130$ mass region. They showed, however, some difficulties in the treatment of pairing correlation, especially when the low-energy positive-parity states exhibited a complex structure [1,33]. As reported by Liden [34] and Hartley [17], using the cranked shell model, the mixed con-

figuration between $9/2^+[404]$ and $3/2^+[422]$ bands in Cs, La, Pr, and Pm is dependent on proton pairing and might due to a residual neutron-proton interaction for high- j intruder bands close to the Fermi surface.

Within deformed shell model, using the Nilsson-Strutinsky procedure [35], the low-energy observed structure in the so-called $A \approx 130$ mass region could be mainly associated with the behavior of the $\pi h_{11/2}$ orbital near the Fermi surface. As reported by Chen *et al.* [22], the nuclear shape might be explained from the opposite driving forces of valence protons, when filling the lower part of the $h_{11/2}$ subshell, and valence neutrons, being at or above the $h_{11/2}$ midshell. Such resulting equilibrium shapes could result from prolate shape, due to protons, and oblate or triaxial shapes, due to neutrons. This coexistence phenomenon was experimentally evidenced by Liang *et al.* [36] to be associated to the same single-quasiproton orbital where the average proton and neutron gamma-driving forces are calculated to be evolving with opposite sign and therefore resulting in the prediction of both low- K ($K = 1/2$) prolate and high- K ($K = 11/2$) oblate minima of similar depths in the potential well, where K is the angular momentum projection on the symmetry axis.

Therefore, it is interesting to tackle the problem of the $\pi g_{7/2}$, $\pi g_{9/2}$, and $\pi h_{11/2}$ bands in the $A \approx 130$ mass region, in order to observe how the proton and neutron Fermi surfaces affect their deformation-driving tendency. We hence used a Soloviev [37] inspired model, the quasiparticle-phonon coupling plus rotor model (QPRM) [38–40]. In this approach we use the deformed Nilsson averaged field where the deformation parameters [41,42] are included to obtain the wave function of the states and the single-particle energies. Nilsson diagrams indicate that the microscopic structure of odd- A

*abdenbikhouaja@gmail.com

nuclei in the mass region of interest is built upon several positive-parity proton orbitals originating from the $\pi g_{7/2}$, $\pi d_{5/2}$, and $\pi g_{9/2}$ spherical shell model states which might determine the low excitation energy structure, whereas for the negative-parity states there is only the $\pi h_{11/2}$ orbital. In many nuclei, however, some of the expected low-energy positive levels have not been observed yet.

The odd-mass system could be treated as an independent quasiparticle motion by the BCS (Bardeen, Cooper, and Schrieffer) approximation [43–46], which allows determining the quasiparticle energies and the occupation probability coefficients of the intrinsic states. Since we are interested in the low-energy level structure, the quadrupolar excitation mode can be studied with the TDA (Tamm-Dancoff approximation) [47]. This approach is microscopic in the sense that it provides two-quasiparticle structure of the quadrupole vibrational core (γ -phonon) in contrast to phenomenological models such as that in Ref. [48] where the question of phonon structure is *a priori* excluded.

The aim of this work is to study the low-energy spectroscopic structure of lanthanum isotopes in a transitional region where a variety of coexisting structures could be revealed between the nearly spherical region and the deformed region. We used QPRM approach, in order to investigate the different deformation-driving properties on the single-proton energy and subsequently occupied subshell (configuration). We explored the low-collectivity of ^{123}La where such effects of pairing, recoil, and quadrupole forces are progressively revealed on the structure of the ground and low-energy excited states, restricted in the very low-energy spectrum within a window less than 1 MeV from the ground-state level. We systematically studied the structural evolution of the ground and low-energy one-quasiproton states for ^{121}Cs , ^{125}Pr , and $^{123,125,127,129}\text{La}$. Prominent results are shown in our assignments of the available observed band structures. The ground state is assigned, and the origin of the excited ones is identified from their corresponding bandheads.

The paper is organized as follows. In Sec. II, we briefly present the Hamiltonian formalism that treats the one-quasiparticle system in terms of intrinsic, rotational, and Coriolis motions. The results of our QPRM calculations are presented in Sec. III. We first study the contribution of Hamiltonians—quadrupolar, recoil, and pairing—on the low-energy structure of ^{123}La for possible ground states close to the Fermi level. We extend our discussions to include the driving-force deformations on the systematic evolution of the low-energy structure along the ^{121}Cs and ^{125}Pr isotonic chains as well as the $^{123,125,127,129}\text{La}$ isotopic chain. Such coexisting structures at low energy are shown to be associated with strong mixture of the positive parity and Coriolis effect for the negative one. Finally, we concluded on the possibilities of our formalism to describe the nuclear structure in the transitional region of the neutron-deficient side.

II. THEORETICAL FORMALISM

Theoretical calculations were carried out for the transitional region $A \approx 130$ using the QPRM approach based on the Nilsson, BCS, and TDA formalisms. Bandheads, like ground

and low-energy excited states, are particularly investigated with the standard assumption of the total Hamiltonian formalism [38–40,49],

$$H = H_{\text{int}} + H_I + H_C, \quad (1)$$

where H_{int} is the intrinsic motion, H_I is the collective kinetic energy associated with the rotation of the nucleus, and H_C is the Coriolis force, which couples the intrinsic and rotational motions. Treating an odd- A nucleus as a system of an extra nucleon coupled to an even-even core, the assumption of an axially symmetric rotor [47] can then reduce the rotational Hamiltonian to

$$H_I = A_R(I^2 - I_3^2) \quad (2)$$

and the Coriolis force to

$$H_C = -A_R(I_+ J_- - I_- J_+) \quad (3)$$

with $I_{\pm} = I_1 \pm iI_2$, $J_{\pm} = J_1 \pm iJ_2$, and $A_R = \frac{\hbar^2}{2\mathfrak{I}}$. Here, \mathfrak{I} is the moment-of-inertia parameter along the two axes $k = 1, 2$ perpendicular to the symmetry axis $k = 3$. The total angular momentum I is composed of two terms: the collective rotation of the core and the angular momentum of the extra nucleon, J .

Considering the BCS and TDA approximations of such an adopted quasiparticle system and the microscopic structure of the γ -phonon state, the intrinsic Hamiltonian H_{int} summarizes the most interesting physical parameters of Nilsson average deformed field H_{sp} [50], monopole pairing interaction H_P [46], and, the residual interactions represented by quadrupole-quadrupole interaction H_Q [47] and recoil force H_J [46]:

$$H_{\text{int}} = H_{sp} + H_P + H_Q + H_J,$$

where

$$\begin{aligned} H_{sp} &= \sum_{\nu\tau} e_{\nu\tau} a_{\nu\tau}^+ a_{\nu\tau}, \\ H_P &= - \sum_{\nu\mu\tau} G_{\tau} a_{\nu\tau}^+ a_{-\nu\tau}^+ a_{-\mu\tau} a_{\mu\tau}, \\ H_Q &= -\frac{1}{2} \chi \sum_{\tau\tau'} \{Q_{22}^+(\tau) Q_{22}(\tau') + Q_{2-2}^+(\tau) Q_{2-2}(\tau')\}, \\ H_J &= \frac{1}{2} A_R \sum_{\tau\tau'} [J_-(\tau) J_+(\tau') + J_+(\tau) J_-(\tau')]. \end{aligned} \quad (4)$$

Here $a_{\nu\tau}^+ a_{\nu\tau}$ is the operator that creates (destroys) a particle of nucleon type τ (neutron or proton) in a Nilsson orbital with energy $e_{\nu\tau}$. The quantum number ν stands for the asymptotic quantum along numbers $[N, n_z, \Lambda]$ with the projection Ω_{ν} of the particle angular momentum along the symmetry axis. The quadrupole moment of mass with $\gamma = \pm 2$ is given as a one-body interaction,

$$Q_{2\gamma}(\tau) = \sum_{\nu\tau\mu} \langle \nu\tau | r^2 Y_{2\gamma} | \mu\tau \rangle a_{\nu\tau}^+ a_{\mu\tau}. \quad (5)$$

Diagonalization of the total Hamiltonian is performed within the basis formed by the symmetrized rotational

functions [46],

$$|IMK\rho\rangle = \sqrt{\frac{2I+1}{16\pi^2}} \{D_{MK}^I |K\rho\rangle + (-)^{I+K} D_{M-K}^I |\bar{K}\rho\rangle\}. \quad (6)$$

Herein ρ is the quantum number of a given intrinsic state with a projection K of the intrinsic angular momentum along the symmetry axis. $|K\rho\rangle$ can be obtained by resolving the secular problem,

$$\begin{aligned} H_{\text{int}}|K\rho\rangle &= (H_{sp} + H_P + H_Q + H_J)|K\rho\rangle \\ &= E_{K\rho}^{\text{int}}|K\rho\rangle. \end{aligned} \quad (7)$$

As is well known, D_{MK}^I is the rotational matrix and is an eigenfunction of I^2 and I_3 with eigenvalues $I(I+1)$ and K , respectively. Thus, for a diagonalization of H within the basis states, Eq. (6) is essentially requiring one to determine the matrix element of the Coriolis term H_C [49],

$$\begin{aligned} &\langle IMK'_\rho | H_C | IMK\rho \rangle \\ &= -A_R \left\{ (-)^{I+\frac{1}{2}} \left(I + \frac{1}{2} \right) \langle K'_\rho | J_+ | \bar{K}\rho \rangle \delta_{K'\frac{1}{2}} \delta_{K\frac{1}{2}} \right. \\ &\quad \left. + \sqrt{(I_\mp K)(I \pm K + 1)} \langle K'_\rho | J_\pm | \bar{K}\rho \rangle \delta_{K',K\pm 1} \right\}. \end{aligned} \quad (8)$$

In the frame of our QPRM approach, configurations for wave functions of the resulting intrinsic state $|K\rho\rangle$ must contain contributions of both one-quasiparticle and quasiparticle-phonon components,

$$|K\rangle = \left(\sum_\nu C_\nu^\rho \delta_{K\nu} \alpha_{\nu\tau}^+ + \sum_{\nu\gamma} D_{\nu\gamma}^\rho \delta_{K=\Omega_\nu+\gamma} \alpha_{\nu\tau}^+ A_\gamma^+ \right) |BCS\rangle. \quad (9)$$

$|BCS\rangle$ is the BCS ground state and $\alpha_{\nu\tau}^+$ represents the creation quasiparticle operator for a nucleon τ . The BCS approach is an approximate approach when treating the pairing correlation by using the Bogoliubov-Valatin transformation which makes change from particle to quasiparticle operators $\alpha_{\sigma\nu\tau}^+ = U_{\nu\tau} \alpha_{\sigma\nu\tau}^+ + \sigma V_{\nu\tau} \alpha_{-\sigma\nu\tau}$.

The quadrupole-phonon operator is defined in the frame of the Tamm-Dancoff approximation (TDA) [47],

$$A_\gamma^+ = \frac{1}{2} \sum_{\nu\mu\tau} (X_\gamma^\tau)_{\nu\mu} \alpha_{\nu\tau}^+ \alpha_{\mu\tau}^+ \quad (10)$$

This expression permits a microscopic structure description for the quadrupole vibrational core (γ -phonon state) by examining the χ amplitudes which are related to two-quasiparticle excitations.

The resolution of Eq. (6) for an odd- A nucleus is perfected by a diagonalization within a basis formed by one-quasiparticle states (1-qp) and quasiparticle-phonon coupling states (qp-ph $_\gamma$). If we only retain the terms that do not have zero matrix elements within the states of this basis, the intrinsic Hamiltonian is then reduced to

$$\begin{aligned} H_{\text{int}} &= H_{BCS} + H_{11}^Q + H_{20}^Q + H_{22}^Q + H_{31}^Q + H_{11}^J + H_{20}^J \\ &\quad + H_{22}^J + H_{31}^J + H_{22}^P. \end{aligned} \quad (11)$$

The Q and J terms are respectively related to quadrupole and recoil forces. The last term H_{22}^P is a residual pairing

interaction, which was neglected in the BCS approximation. The interactions between two (1-qp) and two (qp-ph $_\gamma$) states are given respectively by L_{11} and L_{22} matrix elements and that between (1-qp) and (qp-ph $_\gamma$) states by L_{31} . They are expressed as follows [39,40]:

$$L_{11} = \langle BCS | \alpha_{K'\tau} (H_{BCS} + H_{11}^Q + H_{11}^J) \alpha_{K\tau}^+ | BCS \rangle, \quad (12)$$

$$\begin{aligned} L_{22} &= \langle BCS | A_{\gamma'} \alpha_{K'\tau} (H_{BCS} + H_{11}^Q + H_{11}^J + H_{22}^Q + H_{22}^J \\ &\quad + H_{22}^P) \alpha_{K\tau}^+ A_{\gamma'}^+ | BCS \rangle, \end{aligned} \quad (13)$$

$$L_{31} = \langle BCS | A_\gamma \alpha_{K'\tau} (H_{20}^Q + H_{20}^J + H_{31}^Q + H_{31}^J) \alpha_{K\tau}^+ | BCS \rangle. \quad (14)$$

Therefore, the eigenvalue problem is expressed in matrix form,

$$\begin{pmatrix} L_{11} & L_{31} \\ L_{31} & L_{22} \end{pmatrix} \begin{pmatrix} C_K^\rho \\ D_{K_\gamma}^\rho \end{pmatrix} = E_{K\rho}^{\text{int}} \begin{pmatrix} C_K^\rho \\ D_{K_\gamma}^\rho \end{pmatrix}, \quad (15)$$

where C_K^ρ represents the (1-qp) component and $D_{K_\gamma}^\rho$ represents the (qp-ph $_\gamma$) component. The intrinsic eigenvalue $E_{K\rho}^{\text{int}}$ corresponds to the eigenvector of Eq. (7).

In summary, from the above equations, our theoretical calculations should be processed in two steps. First, the intrinsic eigenvalue of Eq. (7), when solved, gives a set of intrinsic states $|K\rho\rangle$ and intrinsic energies $E_{K\rho}^{\text{int}}$. From the obtained states, different rotational wave functions with the form given in Eq. (6) are constructed. Then, in a second step, a diagonalization of the Coriolis term is performed.

III. RESULTS AND DISCUSSION

In the present work, we used the QPRM approach to systematically investigate the ground and low-energy structures of isotonic ^{121}Cs , ^{125}Pr and isotopic $^{123,125,127,129}\text{La}$ nuclei, where such expected interplays between individual and collective correlations can be explored from weaker pairing. Henceforth, each nucleus of interest is treated as a system of an even-even core plus an extra nucleon, following the standard assumption of Nilsson, BCS, and TDA approximations.

The even-even core structure is reproduced in a deformed average Nilsson field using conjointly the deformation parameters ε_2 covering the large values of 0.2 to 0.275 from Ref. [41] and the adjusted parameters κ and μ (see Table I). The BCS pairing gap is fixed for proton and neutron from the Fermi level energy λ , and by the well-known phenomenological relation $\Delta_p = \Delta_n = 12/A^{1/2}$ MeV [51]. And, for TDA calculations, the parameter of quadrupole force χ is fitted from the experimental energy of the quadrupole vibrational core using the experimental data from [52–57]. As shown in Fig. 1, the vibrational excitation energies are localized at $E(2^+) = 876.09, 618.2,$ and 510 keV for the isotonic chain with cores of ^{120}Xe , ^{122}Ba , ^{124}Ce , and at $E(2^+) = 873.2, 873.5,$ and 884.57 keV for the isotopic chain with cores of ^{124}Ba , ^{126}Ba , and ^{128}Ba , respectively.

The effect of all parameters stated above is summarized in a subroutine diagonalizing the total Hamiltonian, where the inertia parameters are determined semiempirically using the

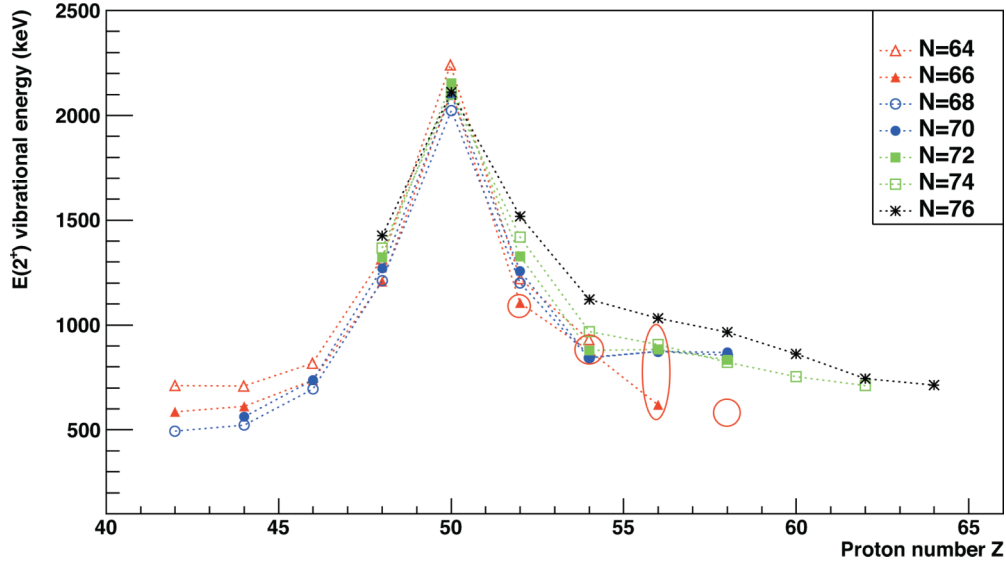


FIG. 1. Experimental vibrational excitation energy $E(2^+)$ for the isotonic chain $N = 64-76$ in the region of $42 \leq Z \leq 64$ [63]. The surrounded points indicate the energy of the even-even core considered by TDA calculations. The excitation energy of ^{124}Ce is obtained by extrapolation from the value of experimental $E(2^+)$.

energy of first excited state $\varepsilon_2^2 \approx 1176[A^{7/3}E(2^+)]^{-1}$ [58,59] and the pairing strength parameters $G_P = 19.6A^{-1}$ and $G_N = [19.6 - 15.7(N - Z)A^{-1}]A^{-1}$ MeV, obtained phenomenologically [60]. In the following subsections, we systematically demonstrated the contributions of Nilsson, BCS, and TDA by studying the available low-energy microscopic structure of ^{123}La .

A. Single-particle energies within Nilsson formalism

According to the deformed shell model, the collective bands—bandheads—of the nuclei of interest should originate from single-proton configurations. In the region of closed

TABLE I. (κ, μ) values of Nilsson potential as a function of Oscillator shell number N for protons and neutrons. The “universal” values of Bengtsson and Ragnarsson [61,62] are given, in comparison to the fitted values (as shown in bold) of the current analysis.

Oscillator shell (N)	Proton				Neutron	
	Standard		Fitted		Standard	
	κ_P	μ_P	κ_P	μ_P	κ_N	μ_N
0	0.120	0.00			0.120	0.00
1	0.120	0.00			0.120	0.00
2	0.105	0.00			0.105	0.00
3	0.090	0.30			0.090	0.25
4	0.065	0.57	0.070	0.44	0.070	0.39
5	0.060	0.65	0.058	0.54	0.062	0.43
6	0.054	0.69			0.062	0.34
7	0.054	0.69			0.062	0.26
8	0.054	0.69			0.062	0.26

shells of $50 \leq Z, N \leq 82$, one can rapidly search for the band assignments from the calculated Nilsson diagram. We therefore studied the single-particle energy as a function of deformation parameter ε_2 between 0.2 and 0.275, where the neutron deficient nuclei ^{121}Cs , ^{125}Pr , and $^{123,125,127,129}\text{La}$ are localized. As presented in Fig. 2, we expected studying the collective bands with an assembly of single-proton configurations originating from $\pi d_{3/2}$, $\pi d_{5/2}$, $\pi f_{5/2}$, $\pi p_{1/2}$, $\pi g_{7/2}$, $\pi g_{9/2}$, $\pi h_{9/2}$, and $\pi h_{11/2}$ subshells.

In Table I, we adjusted the parameters of κ and μ in a way to reproduce the Nilsson orbitals of considered region of nuclei. As a function of oscillator shell number N , the intrinsic eigenvalues and states are shown to be very sensitive to the Nilsson potential according to the values of κ and μ , particularly for $N = 4-5$. We present in Table II the obtained results of our Nilsson calculations for ^{123}La , having ^{122}Ba as even-even core with deformation parameter $\varepsilon_2 = 0.25$. For each Nilsson orbital (column 1), the intrinsic energy is given in $\hbar\omega$ (column 2) and the wave functions (columns 3–6) are calculated for nucleonic motion in the prolate potential. We see from Table II that the eigenstates exhibit strong mixing of components with different Λ values resulting from the deformation. Consequently, for the possible proton intrinsic states near the Fermi level, we only retained the large amplitude of wave function as a function of asymptotic Nilsson components. As listed in Table II, around the Fermi level there are many positive-parity and negative-parity states built upon $1/2^+$, $3/2^+$, $5/2^+$, $7/2^+$, $9/2^+$, $1/2^-$, $3/2^-$, $5/2^-$, and $7/2^-$ orbitals. The origin of such states is known, as shown in bold, from the large amplitude (more than 0.5) of the wave function. Among these states, the collective bands—treated as ground and low-energy excited states—of ^{123}La can feel the dominance of such effects of either weak or strong Coriolis mixing.

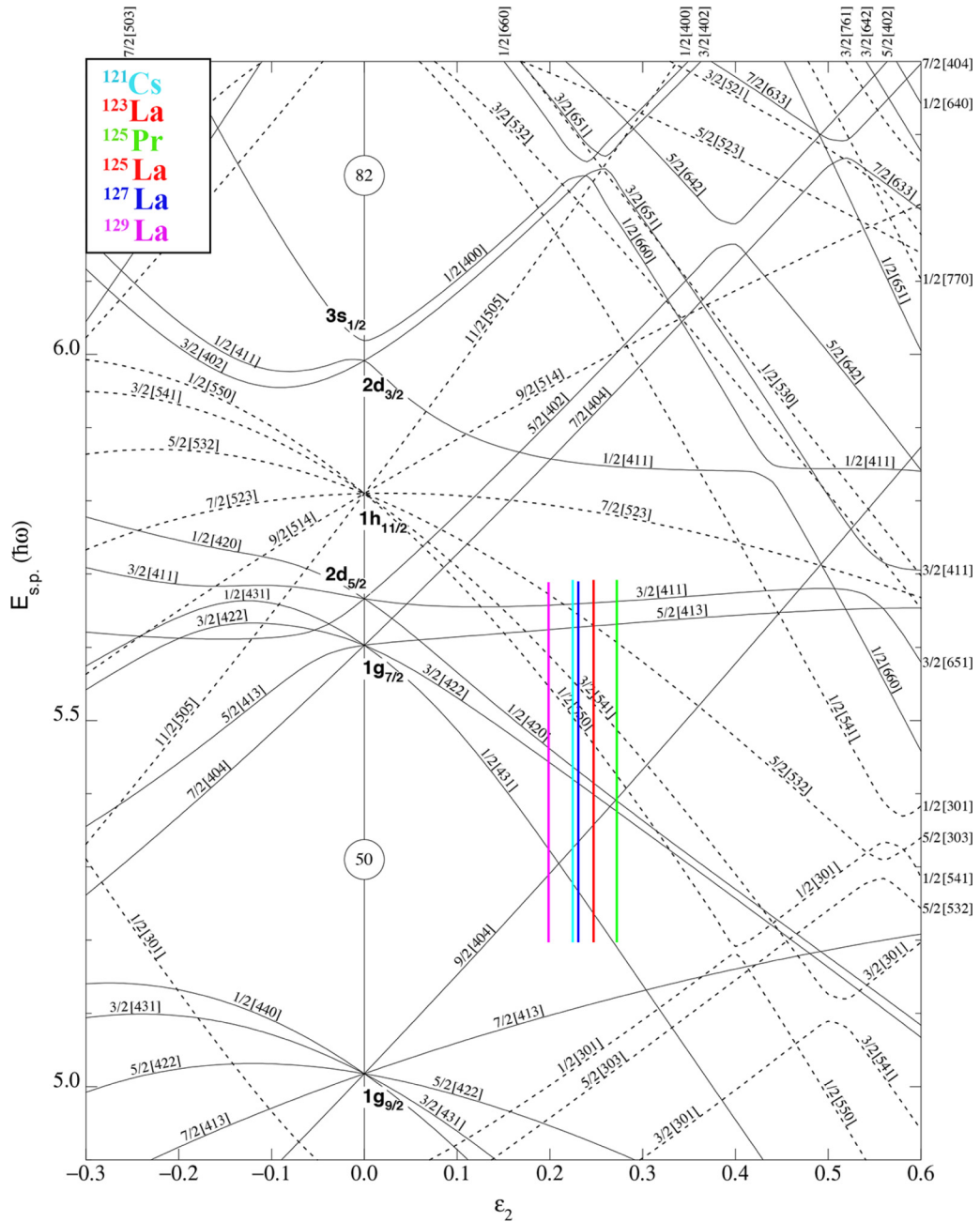


FIG. 2. Nilsson diagram for protons of the closest shells of $50 \leq Z \leq 82$. The different color lines localize, as a function of deformation parameter, the expected core orbitals: light blue for ^{120}Xe ($\epsilon_2 = 0.225$), green for ^{124}Ce ($\epsilon_2 = 0.275$), red for $^{122,124}\text{Ba}$ ($\epsilon_2 = 0.25$), blue for ^{126}Ba ($\epsilon_2 = 0.233$), and pink for ^{128}Ba ($\epsilon_2 = 0.2$).

B. One-quasiparticle states of ^{123}La within BCS formalism

When theoretically studying the ^{123}La nucleus, the extra proton nucleon must be deeply correlated with low and high collectivity of the even-even core nucleus. We have to primarily identify the ground state from excited ones in a region where the excitation gap is rather important. The core ^{122}Ba is well known to have γ -soft deformed structure with lowest energy $h_{11/2}$ proton orbital strongly dealing with quadrupole and octupole correlations [64,65]. This structural effect was observed when establishing the collectivity of ^{122}Ba from low to high spin states, which

showed the existence of four quadrupolar and one octupolar bands [64–67]. However, according to the cranked shell model (CSM) calculations [65], the ground state is mainly supported from the gradual alignment of a configuration of two $h_{11/2}$ quasiprotons. As reported in Ref. [66], the favored signature of proton configuration $\pi h_{11/2}[550]1/2 \otimes \pi g_{7/2}[422]3/2$ is assigned to the second band, while the unfavored one $\pi h_{11/2}[550]1/2 \otimes \pi d_{5/2}[420]1/2$ is assigned to the third band. A strongly coupled fourth band is suggested to be originating from the proton configuration of $\pi g_{9/2}[404]9/2 \otimes \pi h_{11/2}[550]1/2$. The remaining strongly coupled band is suggested to have a configuration of two quasineutrons

TABLE II. Structure of intrinsic states (eigenvalues and intrinsic states of the Hamiltonian with adjusted parameters given in Table I) close to the Fermi level for the ^{122}Ba nucleus. The wave functions are given in the basis of asymptotic quantum numbers $\Omega_{\pi}[N, n_z, \Lambda]$, where Ω is the quantum number that corresponds to the third component of the angular momentum in the intrinsic frame, π and N are the parity and principal quantum number of the major oscillator shell, n_z is the number of quanta associated with the wave function moving along the z direction, and Λ is the projection of the orbital angular momentum onto the z axis (symmetry axis). The retained wave functions are highlighted from their large amplitude.

Nilsson orbital	Particle energy ($\hbar\omega$)	Components of Nilsson on asymptotic base (with the corresponding spherical orbitals)								
		[402]($2d_{3/2}$)	[411]($2d_{5/2}$)	[422]($1g_{7/2}$)	[431]($1g_{9/2}$)	[400]($3s_{1/2}$)	[411]($2d_{3/2}$)	[420]($2d_{5/2}$)	[431]($1g_{7/2}$)	[440]($1g_{9/2}$)
3/2 ⁺ [411]	5.627	-0.178	0.890	0.390					-0.154	
3/2 ⁺ [422]	5.426	0.213	-0.205	0.782					0.548	
3/2 ⁺ [431]	4.775	-0.092	0.327	-0.463					0.818	
1/2 ⁺ [411]	5.819	-0.165	0.863	0.391	-0.220				-0.158	
1/2 ⁺ [420]	5.387	0.213	-0.180	0.758	0.573				-0.131	
1/2 ⁺ [431]	5.210	-0.087	0.341	-0.184	0.551				0.733	
5/2 ⁺ [413]	5.683		[402]($2d_{5/2}$)		[413]($1g_{7/2}$)				[422]($1g_{9/2}$)	
5/2 ⁺ [422]	4.929	-0.160		0.906					0.390	
5/2 ⁺ [402]	5.912	0.187		-0.360					0.914	
		0.969		0.218					-0.110	
7/2 ⁺ [404]	5.972		[404]($1g_{7/2}$)						[413]($1g_{9/2}$)	
7/2 ⁺ [413]	5.129			0.970					0.242	
				-0.242					0.970	
9/2 ⁺ [404]	5.366				[404]($1g_{9/2}$)					
				1.000						
5/2 ⁻ [532]	5.685	[503]($2f_{5/2}$)	[512]($1h_{9/2}$)	[523]($2f_{7/2}$)					[532]($1h_{11/2}$)	
		-0.079	0.314	-0.411					0.851	
		[503]($1h_{9/2}$)		[514]($2f_{7/2}$)					[523]($1h_{11/2}$)	
7/2 ⁻ [523]	5.858	0.180		-0.323					0.929	
		[501]($3p_{1/2}$)	[512]($1h_{9/2}$)	[521]($3p_{1/2}$)	[532]($1h_{11/2}$)				[541]($2f_{7/2}$)	
3/2 ⁻ [541]	5.558	0.068	-0.179	0.443	-0.486				0.728	
		[501]($3p_{1/2}$)	[510]($2f_{5/2}$)	[521]($3p_{1/2}$)	[530]($1h_{9/2}$)	[541]($2f_{7/2}$)	[550]($1h_{11/2}$)			
1/2 ⁻ [550]	5.487	-0.049	0.169	-0.326	0.541	-0.540	0.526			
1/2 ⁻ [541]	6.055	0.074	-0.052	0.420	0.126	0.542	0.710			

of $\nu h_{11/2}[523]7/2 \otimes \nu d_{5/2}[402]5/2$ and/or $\nu h_{11/2}[523]7/2 \otimes \nu g_{7/2}[413]5/2$. Moreover, from the systematics of low-energy γ bands, heavier barium isotopes are expected to present a considerable degree of γ softness [68], where such effect could be manifested with considerable energy staggering in the sequence of γ bands. ^{122}Ba is considered a good candidate of large degree γ softness since the second even-spin (2^+) state is observed at 618.2 keV [67].

We therefore studied the low collectivity of core ^{122}Ba by introducing the BCS approach, in which the correlation between quasiparticle operators (creation and annihilation) is well determined. With this approach, we numerically treated the energy of 20 Nilsson orbitals equally positioned both below and above the Fermi level, which are candidates to build up the ground state as cited above. In Table III, we presented for each level the calculated energy, as well as its occupancy (U) and vacancy (V) probabilities, for both protons (A) and neutrons (B), respectively. We noticed that when looking for

the closest energy level to the Fermi one, the decision to choose the ground state only based on the energy cannot be unambiguous.

C. One-quasiparticle states of ^{123}La within TDA approximation

Within the TDA formalism, the ^{123}La nucleus is simply treated from the two-body interaction, where the shape softness of ^{123}La can be introduced and strongly affected from the core ^{122}Ba , in a dynamic manner by γ vibration [see Eq. (10)]. In Table IV (column 5), the amplitude values $(\chi_{\gamma})_{\mu\nu}$ of TDA phonons have been calculated for different combinations of states around the Fermi level. We indicate, with double asterisks, the largest vibration amplitudes which could yield optimal configuration states ($\pi g_{7/2}[422]3/2^+$, $\pi d_{5/2}[420]1/2^+$), ($\pi h_{11/2}[541]3/2^-$, $\pi h_{11/2}[550]1/2^-$), and ($\pi h_{11/2}[532]5/2^-$, $\pi h_{11/2}[550]1/2^-$) for protons as well as, for neutrons, ($\nu g_{7/2}[411]3/2^+$,

TABLE III. Quasiparticle energy levels calculated for ^{122}Ba around the Fermi surface. The closest energies to the Fermi level are shown in bold.

A. Proton case				B. Neutron case			
Bandhead levels	Energy levels (MeV)	U	V	Band head levels	Energy levels (MeV)	U	V
$3/2^+[431]$	5.944	0.091	0.996	$7/2^+[413]$	5.356	0.101	0.995
$3/2^-[301]$	5.311	0.102	0.994	$1/2^+[431]$	4.951	0.110	0.993
$5/2^+[422]$	4.690	0.116	0.993	$1/2^+[420]$	3.469	0.158	0.988
$5/2^-[303]$	4.139	0.132	0.991	$9/2^+[404]$	3.446	0.159	0.987
$1/2^-[301]$	3.806	0.144	0.989	$3/2^+[422]$	3.089	0.178	0.983
$7/2^+[413]$	3.091	0.178	0.984	$1/2^-[550]$	2.554	0.217	0.976
$1/2^+[431]$	2.465	0.226	0.974	$3/2^-[541]$	1.989	0.284	0.958
$9/2^+[404]$	1.399	0.430	0.902	$3/2^+[411]$	1.728	0.333	0.942
$1/2^+[420]$	1.289	0.480	0.877	$5/2^+[413]$	1.253	0.500	0.865
$3/2^+[422]$	1.141	0.589	0.808	$5/2^-[532]$	1.205	0.532	0.846
	Fermi level	5.449			Fermi level	5.754	
$1/2^-[550]$	1.107	0.772	0.634	$1/2^+[411]$	1.125	0.794	0.607
$3/2^-[541]$	1.385	0.900	0.435	$7/2^-[523]$	1.522	0.922	0.386
$3/2^+[411]$	1.815	0.948	0.315	$5/2^+[402]$	1.556	0.926	0.376
$5/2^+[413]$	2.212	0.967	0.253	$7/2^+[404]$	2.258	0.968	0.248
$5/2^-[532]$	2.233	0.967	0.251	$1/2^-[541]$	2.741	0.979	0.202
$1/2^+[411]$	3.259	0.985	0.169	$9/2^-[514]$	3.049	0.983	0.181
$7/2^-[523]$	3.565	0.988	0.154	$1/2^+[400]$	3.540	0.988	0.155
$5/2^+[402]$	4.000	0.990	0.137	$3/2^+[402]$	3.811	0.989	0.144
$7/2^+[404]$	4.382	0.992	0.122	$1/2^-[530]$	3.843	0.989	0.142
$1/2^-[541]$	5.159	0.994	0.106	$3/2^-[532]$	4.148	0.991	0.132

$\nu s_{1/2}[411]1/2^+$, $(\nu d_{5/2}[413]5/2^+$, $\nu s_{1/2}[411]1/2^+$), and $(\nu h_{11/2}[523]7/2^-$, $\nu h_{11/2}[541]3/2^-)$. Herein, the low collectivity of the core could be resumed in a structure of ground and excited states assigned with a sequence of positive even spins 0^+ , 2^+ , etc. Consequently, the extra-proton nucleus may be correlated with an even-even core, presenting an equilibrium between vibrational and/or rotational interactions. From Table III, we can learn that the final structure of ^{123}La should be mostly adopted from the single-proton configurations originating from $\pi d_{5/2}$, $\pi g_{7/2}$, $\pi g_{9/2}$, and $\pi h_{11/2}$ subshells, which were previously suggested to be near the Fermi surface at $Z = 57$ [69]. This is true when we only consider the BCS and TDA calculations without the contributions of recoil force and quadrupole and residual pairings to the intrinsic Hamiltonian [Eq. (11)]. However, with our QPRM calculations, the ground and low-energy structure of such nucleus is established when including the multiple contributions of the intrinsic Hamiltonian to the energy of resulting intrinsic states, assigned by the dominant one-quasiparticle configuration (see Fig. 3).

D. One-quasiparticle states in ^{123}La within QPRM formalism

The odd ^{123}La nucleus was observed with lowest (ground) state assigned by $5/2^+$ [28]. Six rotational bands, with linked transitions, were identified from low to high spins [28,69] and built upon the Nilsson orbitals $3/2^+[422]$, $1/2^-[550]$, $3/2^-[541]$, $1/2^+[420]$, $9/2^+[404]$, which were firmly and/or tentatively assigned from the cranked shell model calculations and the directional angular correlations of oriented states (DCO) analysis. The $3/2^+[422]$ band is built from the lowest

$3/2^+$ state observed at 35.4 keV from the proposed ground state. Close to the Fermi surface, the Nilsson orbital labeled $1/2^-[550]$ is identified with the lowest bandhead $11/2^-$ level which lies at 4 keV above the bandhead of the first band. From Ref. [28], a high multipolarity (perhaps $E3$) is proposed for the $11/2^-$ bandhead since a transition of low energy, 40 keV, is observed decaying to the proposed ground state, and such β decay from this level is certainly possible [70]. The strongly coupled band labeled $9/2^+[404]$ is assigned $9/2^+$ bandhead spin and parity. The latter was proposed as isomeric state since no linking transitions were observed between this structure and the other neighboring bands [28]. Between the two first bands, a fourth band is observed with lowest energy state assigned to $21/2^+$ at 1797.9 keV suggesting three-quasiparticle configurations. The alignment behavior of this band revealed a configuration similar to the first band without linked transitions, which favored the assignment of $1/2^+[420]$ originating from the component of the $\pi d_{5/2}$ orbital. Furthermore, the last two bands, $1/2^-[550]$ and $3/2^-[541]$, were suggested to present quasi- γ -vibrational structure based on $\pi h_{11/2}$ configuration observed with lowest states $15/2^-$ and $21/2^-$ observed at 957.1 and 1735.5 keV, respectively.

In the present work, we investigated the ground and low-energy excited state bandheads of the ^{123}La nucleus. We present in Fig. 3 the results of our QPRM calculations in comparison to the available experimental data from Refs. [28,69,71]. We show from BCS and TDA calculations an assembly of bands based on candidate bandheads near the Fermi surface, with Nilsson orbital configurations labeled $1/2^-[550]$, $3/2^+[422]$, $1/2^+[420]$, $3/2^-[541]$, $9/2^+[404]$,

TABLE IV. TDA calculations for ^{122}Ba . χ is the amplitude of each couple of orbitals. Each couple is identified by the excitation energy $E_\nu + E_{\nu'}$ and the quadrupole moment of mass. The retained orbitals are highlighted in simple/double asterisks corresponding to the largest quadrupolar amplitude and the smallest excitation energy.

A. Proton case					B. Neutron case				
$\langle \nu $	$ \nu'\rangle$	$\langle \nu r^2 Y_{22} \nu'\rangle$	$E_\nu + E_{\nu'}$	$ \chi $	$\langle \nu $	$ \nu'\rangle$	$\langle \nu r^2 Y_{22} \nu'\rangle$	$E_\nu + E_{\nu'}$	$ \chi $
3/2 ⁺ [431]	1/2 ⁺ [431]	0.581	8.409	0.017	3/2 ⁺ [422]	1/2 ⁺ [431]	0.189	8.041	0.005
3/2 ⁺ [431]	1/2 ⁺ [420]	0.138	7.234	0.008	3/2 ⁺ [422]	1/2 ⁺ [420]	0.951	6.559	0.040
3/2 ⁺ [431]	1/2 ⁺ [411]	0.117	9.204	0.010	3/2 ⁺ [422]	1/2 ⁺ [411]	0.206	4.215	0.038
3/2 ⁻ [301]	1/2 ⁻ [301]	1.340	9.118	0.029	3/2 ⁺ [422]	1/2 ⁺ [400]	0.126	6.630	0.016
3/2 ⁻ [301]	1/2 ⁻ [550]	0.004	6.419	0.001	3/2 ⁻ [541]	1/2 ⁻ [550]	0.779	4.544	0.073
3/2 ⁻ [301]	1/2 ⁻ [541]	0.051	10.471	0.004	3/2 ⁻ [541]	1/2 ⁻ [541]	0.585	4.731	0.107
3/2 ⁺ [422]	1/2 ⁺ [431]	0.062	3.605	0.012	3/2 ⁻ [541]	1/2 ⁻ [530]	0.119	5.833	0.017
3/2⁺[422]	1/2⁺[420]	0.955	2.430*	0.361**	3/2 ⁺ [411]	1/2 ⁺ [431]	0.288	6.680	0.016
3/2 ⁺ [422]	1/2 ⁺ [411]	0.092	4.400	0.016	3/2 ⁺ [411]	1/2 ⁺ [420]	0.024	5.197	0.002
3/2 ⁻ [541]	1/2 ⁻ [301]	0.003	5.192	0.001	3/2⁺[411]	1/2⁺[411]	1.322	2.854*	0.426**
3/2⁻[541]	1/2⁻[550]	0.812	2.493*	0.298**	3/2 ⁺ [411]	1/2 ⁺ [400]	0.016	5.269	0.002
3/2 ⁻ [541]	1/2 ⁻ [541]	0.512	6.545	0.034	3/2 ⁺ [402]	1/2 ⁺ [431]	0.036	8.763	0.003
3/2 ⁺ [411]	1/2 ⁺ [431]	0.327	4.280	0.067	3/2 ⁺ [402]	1/2 ⁺ [420]	0.137	7.280	0.016
3/2⁺[411]	1/2⁺[420]	0.059	3.104*	0.017	3/2 ⁺ [402]	1/2 ⁺ [411]	0.057	4.936	0.007
3/2 ⁺ [411]	1/2 ⁺ [411]	1.327	5.074	0.106	3/2 ⁺ [402]	1/2 ⁺ [400]	1.708	7.350	0.057
5/2 ⁺ [422]	1/2 ⁺ [431]	0.350	7.155	0.013	3/2 ⁻ [532]	1/2 ⁻ [550]	0.285	6.702	0.036
5/2 ⁺ [422]	1/2 ⁺ [420]	0.849	5.979	0.070	3/2 ⁻ [532]	1/2 ⁻ [541]	0.170	6.890	0.006
5/2 ⁺ [422]	1/2 ⁺ [411]	0.077	7.949	0.008	3/2 ⁻ [532]	1/2 ⁻ [530]	0.966	7.992	0.027
5/2 ⁻ [303]	1/2 ⁻ [301]	1.207	7.946	0.034	7/2 ⁺ [413]	3/2 ⁺ [422]	0.434	8.446	0.011
5/2 ⁻ [303]	1/2 ⁻ [550]	0.001	5.247	0.001	7/2 ⁺ [413]	3/2 ⁺ [411]	1.097	7.085	0.055
5/2 ⁻ [303]	1/2 ⁻ [541]	0.028	9.299	0.002	7/2 ⁺ [413]	3/2 ⁺ [402]	0.032	9.167	0.003
7/2 ⁺ [413]	3/2 ⁺ [431]	0.423	9.036	0.010	9/2 ⁺ [404]	5/2 ⁺ [413]	0.327	4.699	0.038
7/2 ⁺ [413]	3/2 ⁺ [422]	0.320	4.232	0.048	9/2 ⁺ [404]	5/2 ⁺ [402]	1.365	5.002	0.230
7/2 ⁺ [413]	3/2 ⁺ [411]	1.127	4.907	0.197	5/2 ⁺ [413]	1/2 ⁺ [431]	0.303	6.205	0.024
9/2 ⁺ [404]	5/2 ⁺ [422]	0.266	6.089	0.019	5/2 ⁺ [413]	1/2 ⁺ [420]	0.016	4.722	0.002
9/2⁺[404]	5/2⁺[413]	0.228	3.611*	0.056	5/2⁺[413]	1/2⁺[411]	1.186	2.378*	0.506**
9/2 ⁺ [404]	5/2 ⁺ [402]	1.382	5.399	0.209	5/2 ⁺ [413]	1/2 ⁺ [400]	0.149	4.793	0.025
5/2 ⁺ [413]	1/2 ⁺ [431]	0.334	4.677	0.062	5/2⁻[532]	1/2⁻[550]	0.690	3.759*	0.117
5/2⁺[413]	1/2⁺[420]	0.036	3.350*	0.010	5/2⁻[532]	1/2⁻[541]	0.441	3.947*	0.094
5/2 ⁺ [413]	1/2 ⁺ [411]	1.167	5.471	0.075	5/2 ⁻ [532]	1/2 ⁻ [530]	0.783	5.048	0.122
5/2 ⁻ [532]	1/2 ⁻ [301]	0.002	6.039	0.001	5/2 ⁺ [402]	1/2 ⁺ [431]	0.580	6.501	0.004
5/2⁻[532]	1/2⁻[550]	0.731	3.340*	0.164**	5/2 ⁺ [402]	1/2 ⁺ [420]	0.	5.025	0.033
5/2 ⁻ [532]	1/2 ⁻ [541]	0.145	7.390	0.005	5/2⁺[402]	1/2⁺[411]	0.049	2.681*	0.016
7/2 ⁻ [523]	3/2 ⁻ [301]	0.037	8.877	0.003	5/2 ⁺ [402]	1/2 ⁺ [400]	1.694	5.096	0.148
7/2 ⁻ [523]	3/2 ⁻ [541]	0.616	4.951	0.061	7/2⁻[523]	3/2⁻[541]	0.580	3.512*	0.151**
5/2 ⁺ [402]	1/2 ⁺ [431]	0.034	6.465	0.004	7/2 ⁻ [523]	3/2 ⁻ [532]	0.428	5.670	0.033
5/2 ⁺ [402]	1/2 ⁺ [420]	0.227	5.289	0.034	7/2 ⁺ [404]	3/2 ⁺ [422]	0.212	5.348	0.035
5/2 ⁺ [402]	1/2 ⁺ [411]	0.091	7.259	0.003	7/2 ⁺ [404]	3/2 ⁺ [411]	0.026	3.986	0.006
7/2 ⁺ [404]	3/2 ⁺ [431]	0.029	10.427	0.002	7/2 ⁺ [404]	3/2 ⁺ [402]	1.399	6.069	0.075
7/2 ⁺ [404]	3/2 ⁺ [422]	0.233	5.623	0.030	9/2 ⁻ [514]	5/2 ⁻ [532]	0.441	4.254	0.086
7/2 ⁺ [404]	3/2 ⁺ [411]	0.020	6.297	0.001					

3/2⁺[411], 1/2⁺[411], and 5/2⁺[413]. Without the correcting terms of the intrinsic Hamiltonian [Eq. (11)] at low excitation energy, at first view the ground state of ^{123}La could be expected from the 1/2⁻[550] orbital, assigned by the 11/2⁻ state, coming up from the Nilsson $\pi h_{11/2}$ subshell. This configuration could be explained from the modified oscillator potential where the high- j intruder orbital is pushed down in energy due to the angular momentum l^2 (μ) and the spin-orbit interaction $l \cdot s$ (κ) terms.

As reported in earlier works [38–40], the ability of our QPRM approach when studying the low-energy structure

of transitional region $A \approx 100, 130, 170$ is demonstrated by introducing the contribution of each term of the intrinsic Hamiltonian [Eq. (11)] to the energy of the intrinsic states, assigned by the dominant one-quasiparticle configuration. Here, as we can see in Fig. 3, by successively adding the quadrupole and recoil forces to the pairing interaction, the spectroscopy scheme at low energy (close to the Fermi surface) could be adjusted and reasonably well compared to the available experimental data [28,69,71]. We therefore concluded that, with the quadrupole force, both one- and two-body terms enabled an important interaction for positive parity states associated

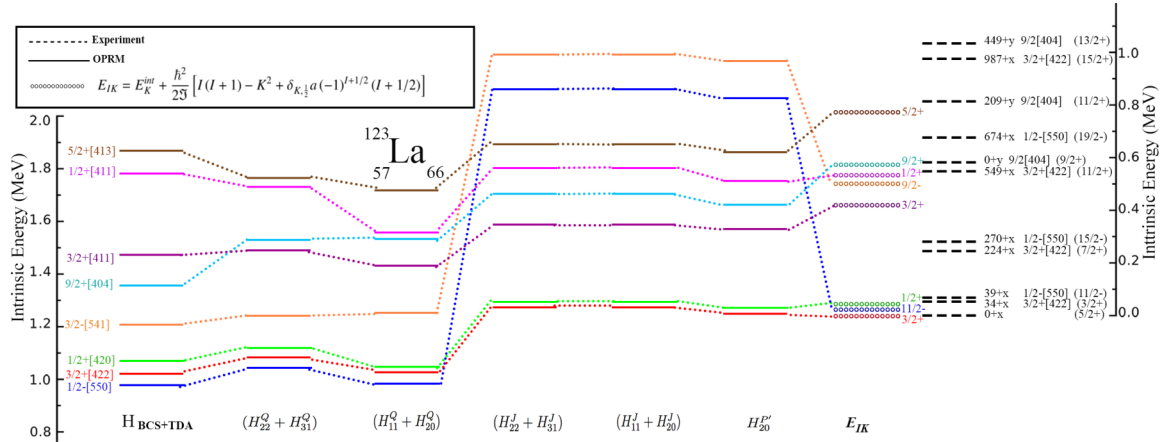


FIG. 3. Intrinsic states of ^{123}La showing the contribution of successive addition of different terms of quadrupole (with index Q), recoil (J), and residual pairing (P) forces to the initial pairing interaction. For orientation, the dashed lines connect the states characterized by the same asymptotic quantum numbers $\Omega_{\pi}[N, n_z, \Lambda]$, as commented in Table II.

with deformation effects, where the energy gap (pairing field) is either relatively increased for the $9/2^+[404]$ or gradually reduced for the $1/2^+[411]$ and $5/2^+[413]$ proton orbitals. The same behavior is remarkably pronounced when adding the recoil force and pairing effects to the previous result. Overall, all forces smoothly influence the proton states belonging to the $N = 4$ oscillator shell.

Coriolis effect and low-energy collectivity

However, as we remarkably see in Fig. 3 for negative parity states belonging to the $N = 5$ oscillator shell, a sudden increase is observed toward large excitation energy when adding the recoil force effect. According to Fig. 2, the protons in the region of interest occupy the states that belong to the $N = 4$ shell and begin filling the $\pi h_{11/2}$ intruder orbitals from $N = 5$. As indicated in Ref. [64], these intruder orbitals polarize the core towards large deformations (oblate or prolate), and, as a consequence, the features of low-energy states of odd nuclei are mostly determined from the angular momentum (j) of the extra nucleon coupled to the axially symmetric nuclear core. Furthermore, two possible extreme coupling (deformation and rotation alignment) forms are illustrated (see Fig. 11.3 in Ref. [42,72]). In the case of strong deformation coupling and slow rotation, the nucleus may deal with small angular momenta of I and j . The projections of j and I on the symmetry axis Ω and K , respectively, are equal, and they are considered conserved quantum numbers, as prominently shown for positive parity states in Fig. 3. However, in the case of weak coupling, the rotation is fast and the strong Coriolis may couple large j (large I) with the collective rotation of the core. This is the case for the high- j neutron and proton orbitals that belong to the $i_{13/2}$ and $h_{11/2}$ subshells where they are uncoupled from the surrounding orbitals of different parity [42], especially when La isotopes are observed with Fermi level situated around the $1/2^- [550]$ orbital with $j \approx 11/2$ and form rotation aligned bands starting with $I = 11/2$.

In our QPRM calculations, since we focused on studying the low-energy one-quasiparticle structure, we adopted the

strong deformation alignment where the collective motion is expressed from the rotational Hamiltonian of Eqs. (2), (3), and (4). We further included the contribution of rotational energy as [42,73]

$$E_{IK} = E_K^{\text{int}} + \frac{\hbar^2}{2\mathcal{I}} [I(I+1) - K^2 + \delta_{K, \frac{1}{2}} a (-1)^{I+1/2} (I+1/2)], \quad (16)$$

where a is the so-called decoupling parameter, which has a fixed value for each $\Omega = 1/2$ orbital, and $\delta_{K, \frac{1}{2}} = 1$, if $K = 1/2$. As $I \geq K$, we only considered the lowest energy among the members of the band that have the spins $I = K, K+1, K+2, \dots$

Consequently, as we can notice from Fig. 3, the effective moment of an odd nucleus is significantly influenced by the polarization of the core produced by the extra particle. The large strength of Coriolis interaction is more pronounced for large angular momentum (j) which, when aligned along the rotation axis, may lead to a minimization of the total energy. Thus, such sudden behaviors are clearly observed for the negative states originating from the $\pi h_{11/2}$ orbitals and smoothly improved for the positive ones. Our theoretical results (the excited states referred to as the corresponding ground states) are plotted in comparison to the available experimental data below the 1-MeV energy window of the plot. We then have an assigned spin and parity proton configuration of $N = 5$ for states $3/2^- [541]$ and $1/2^- [550]$ that originate from the $\pi h_{11/2}$ subshell, and $N = 4$ for states $3/2^+ [422]$ and $5/2^+ [413]$ that originate from the $\pi g_{7/2}$ subshell, $1/2^+ [420]$ and $3/2^+ [411]$ that originate from the $\pi d_{5/2}$ subshell, $1/2^+ [411]$ that originate from the $\pi d_{3/2}$ subshell, and finally $9/2^+ [404]$ that originate from the $\pi g_{9/2}$ subshell.

E. Spin-parity assignment of one-quasiparticle states in ^{123}La

With the present data of our calculations (plotted in Fig. 3) and, when looking at the energy-level sequence, we found close to the Fermi surface a strong mixture of three different configurations, where we could expect the lowest-energy ground state to be assigned by $3/2^+ [422] 3/2^+$ and nearby

excited states of $1/2^- [550]11/2^-$ and $1/2^+ [420]1/2^+$ localized at 10.5 keV and 17.8 keV, respectively. And, the other spaced excited states of $3/2^+ [411] 3/2^+$, $3/2^- [541]9/2^-$, $1/2^+ [411]1/2^+$, $9/2^+ [404]9/2^+$, and $5/2^+ [413]5/2^+$ are, respectively, localized at 409, 489.4, 527.3, 583.2, and 811.7 keV.

At first view, our supposed ground state seems to be in disagreement with the observed experimental one, where ^{123}La is suggested with lowest ground $5/2^+$ state and close low-energy states of $3/2^+$ and $11/2^-$, respectively localized at 35.4 and 39.5 keV [71]. However, this could be explained from Fig. 3, where the low-energy excited states are plotted from the ground ones following Eq. (16). From our calculations, the $5/2^+$ state is presented as an excited state for both $3/2^+ [422]$ and $1/2^+ [420]$ configurations. As reported in Ref. [69], these two bands are known to have strong mixture at low K , which makes it energetically difficult to distinguish them and/or to scale the level-energy between the corresponding transitions. Nevertheless, if β/EC decay were studied for this nucleus, some improvements could be well investigated with the intent to identify the ground state from the possible transitions that might happen with the lowest neighboring bandheads, especially when an $E3$ transition is proposed for the $11/2^-$ bandhead [28,70].

Furthermore, the lack of data makes it difficult to study many bandheads treated in our calculations which were not seen yet experimentally and where the detailed nuclear structure seems to sensitively depend on the relative position of the single-particle levels. We tentatively needed to fix such findings by studying the isotonic behavior of the considered odd- A nucleus ^{123}La , where it is expected to be observed, with similar spectroscopic schemes in the neighboring nuclei (isotones with $N = 66$).

1. One-quasiparticle isotonic systematic trend $N = 66$

Previous experimental findings have assigned the ground states of ^{121}Cs and ^{125}Pr to $3/2^+$, originating from $3/2^+ [422]$ proton Nilsson configuration [14,34]. It was also reported that five rotational bands are unambiguously identified from $(\pi g_{7/2})3/2^+ [422]$, $(\pi d_{5/2})1/2^+ [420]$, $(\pi h_{11/2})1/2^- [550]$, and $(\pi g_{9/2})9/2^+ [404]$ bandhead states. We therefore investigated the isotonic chain of $N = 66$ (^{121}Cs , ^{123}La , and ^{125}Pr) by our QPRM approach using the deformation parameters given by Moller *et al.* [41].

As seen in Fig. 4, for each given isotonic nucleus of the isotonic chain of ^{121}Cs , ^{123}La , and ^{125}Pr , the excited states, characterized by their asymptotic quantum numbers based upon the considered bandhead orbitals, are relative to the corresponding low-energy ground states. The calculated low-energy levels are then compared to the available experimental data. From the lowest energy of calculated levels, we therefore carefully assigned the ground states of ^{121}Cs , ^{123}La , and ^{125}Pr isotones to be commonly represented by the $3/2^+ [422]3/2^+$ state that originates from the $\pi g_{7/2}$ orbital, which somehow is an exception to the suggested observation of a low-energy $5/2^+$ state in ^{123}La [28,69]. Further, as reported near the Fermi surface [34], a subtle balance (mixing) is indicated between the $9/2^+ [404]$, $1/2^+ [420]$, and $3/2^+ [422]$ orbitals, where the

detailed nuclear structure is very sensitive to the position of the single-particle levels. This is indeed apparent from the present bandhead calculations where the corresponding bandheads are all low energy, with 600 keV from the ground state. For the lowest band energy, the calculations showed a strong mixing between $\pi g_{7/2}$ and $\pi d_{5/2}$ orbitals, where the lowest states $3/2^+$ and $1/2^+$ are nearly localized. The strong pairing effect is also clearly indicated for the $\pi g_{9/2}$ orbital which was experimentally suggested to be very close to the Fermi surface for Cs isotopes and higher for La and Pr isotopes [34]. On the other hand, the tendency of the $\pi h_{11/2}$ orbital is observed driving towards larger deformation and becoming lower in energy when increasing the proton number.

For convenience, we also plotted the rotational band members, as low-energy excited states calculated using Eq. (16), for each supposed bandhead, even though this is not the subject of this work since we are only interested in the systematics of ground states. The rotational parameter $\frac{\hbar^2}{2\mathcal{I}}$ was semiempirically adjusted from the inertia parameter and the first excited state of the core nucleus [58,59]. As a result, $\frac{\hbar^2}{2\mathcal{I}} = 43.7, 36.6, \text{ and } 29.6$ keV were commonly obtained for all low-energy expected level bands of ^{121}Cs , ^{123}La , and ^{125}Pr , respectively. We therefore compared our predicted results which, when looking at the position sequence of single-particle levels, especially the rotational band members of $3/2^+ [422](3/2^+, 7/2^+, 11/2^+)$, $1/2^- [550](7/2^-, 11/2^-, 15/2^-, 19/2^-)$, and $9/2^+ [404](9/2^+, 11/2^+, 13/2^+)$, are in reasonable agreement with the available data from Refs. [14,28,34]. Within the framework of our calculations, we tentatively located the bandhead states of $3/2^+ [422]$, $1/2^- [550]$, and $9/2^+ [404]$ at $E(3/2^+) = 0$ keV, $E(11/2^-) = 309.43$ keV, and $E(9/2^+) = 298.45$ keV for ^{121}Cs , $E(3/2^+) = 0$ keV, $E(11/2^-) = 27$ keV, and $E(9/2^+) = 500$ keV for ^{123}La , and at $E(3/2^+) = 0$ keV, $E(7/2^-) = 162.31$ keV, and $E(9/2^+) = 540$ keV for ^{125}Pr , respectively. These lowest states are, respectively, observed from in-beam experiments at $E(3/2^+) = 0$ keV, $E(11/2^-) = 200$ keV, and $E(9/2^+) = 68.5$ keV for ^{121}Cs , $E(3/2^+) = 35$ keV, $E(11/2^-) = 39$ keV, and the scaled $E(9/2^+) = 500$ keV for ^{123}La , and at $E(3/2^+) = 0$ keV, the scaled $E(7/2^-) = 162.31$ keV, and the scaled $E(9/2^+) = 540$ keV for ^{125}Pr . However, some discrepancies can be observed between the calculated and in-beam energy for first excited levels, which are due to the rotational parameter that we did not singly scale to the energy of in-beam bands. We have meanwhile learned that if we carefully adjust the rotational energy, we can easily assign the $1/2^+ [420]5/2^+$ state to the observed low-energy $5/2^+$ state in ^{123}La , since the two $\pi g_{7/2}$ and $\pi d_{5/2}$ orbitals are strongly mixed and the first excited $5/2^+$ of the $(\pi d_{5/2})1/2^+ [420]$ band could potentially occupy the lowest energy.

From this systematic chain, we suggest assigning the observed low-energy bandhead states from $(\pi g_{7/2})3/2^+ [422]$, $(\pi d_{5/2})1/2^+ [420]$, $(\pi h_{11/2})1/2^- [550]$, and $(\pi g_{9/2})9/2^+ [404]$ Nilsson configurations. Otherwise, the unobserved calculated bandhead states are plotted together to enrich the level scheme, awaiting further experimental observations. At this stage of the paper, it appears premature to compare our predictions in terms of excited energy.

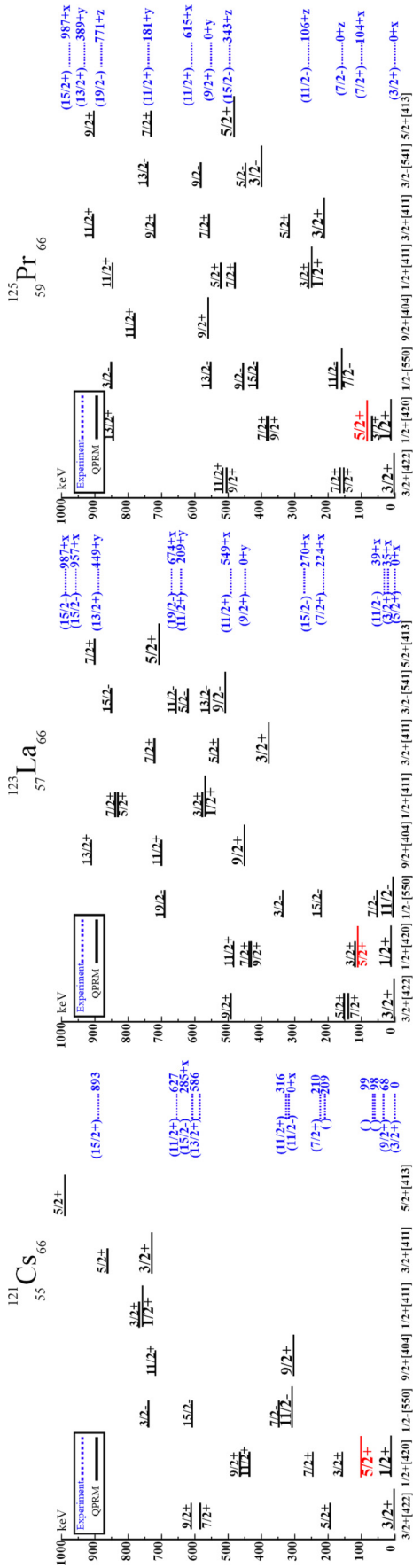


FIG. 4. Low-energy spectroscopic schemes for isotopic nuclei of ^{121}Cs (left), ^{123}La (middle), and ^{125}Pr (right). The calculated levels using the QPRM approach are compared to the available experimental data from [71,74,75].

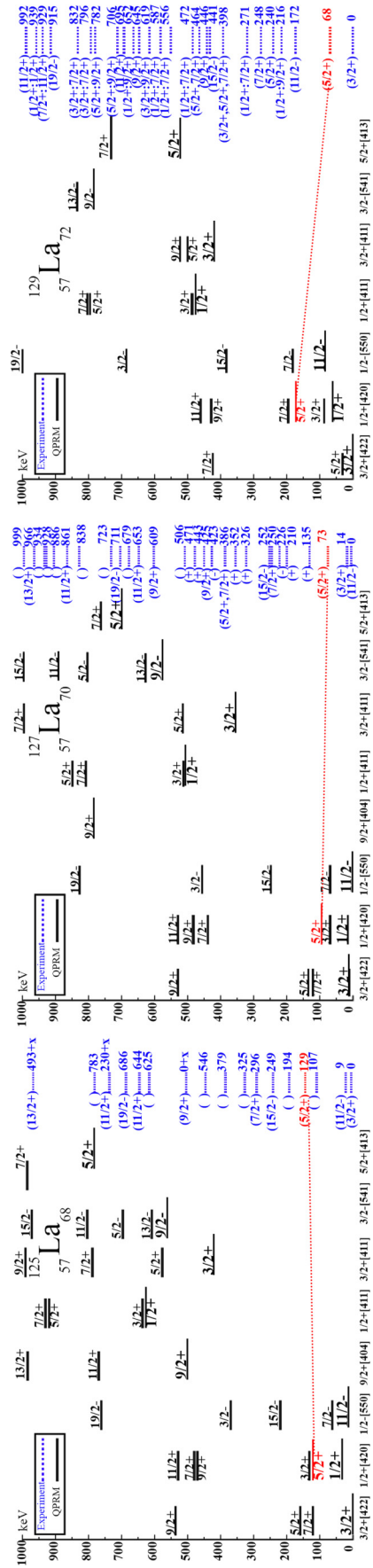


FIG. 5. Low-energy spectroscopic schemes for isotopic nuclei of ^{125}La (left), ^{127}La (middle), and ^{129}La (right) compared to the available experimental data from [75,78,79]. In red, the first excited state of the $1/2^+[420]$ band is connected to the isotopic chain.

The idea, however, was to track the structural evolution of the ground and excited one-quasiparticle states along the considered isotonic chain. Such findings could also be well evidenced when we further study the systematics of the isotopic chain, especially when the assignment of $1/2^+[420]5/2^+$ state is needed along the lanthanum isotopic chain.

2. Isotopic systematic trend of $1/2^+[420]$ band in $^{123,125,127,129}\text{La}$

We followed the same procedure, as presented above for ^{123}La , to perform QPRM calculations for the isotopic chain of $^{125,127,129}\text{La}$ in which we used the quadrupole deformation parameter $\varepsilon_2 = 0.250, 0.233, \text{ and } 0.200$, and the rotational parameter $\frac{\hbar^2}{2\mathcal{I}} = 36.9, 41.9, \text{ and } 50.27$ keV, respectively. We plotted in Fig. 5 the calculated low-energy level schemes for lanthanum isotopes in the mass region $A = 123\text{--}129$, where we could easily assign the lowest-energy ground states as $3/2^+[422]3/2^+$ for ^{125}La , $11/2^-[550]1/2^-$ for ^{127}La , and $3/2^+[422]3/2^+$ for ^{129}La , in comparison to the available experimental data from Refs. [1,3,6,12–14,17,18,28,34,69,76]. As provided by our calculations, the strong mixture between $\pi g_{7/2}$, $\pi d_{5/2}$, and $\pi h_{11/2}$ orbitals still persists at lowest energy, even when increasing the neutron number or decreasing the deformation. Otherwise, the systematics of low-energy levels revealed such effect of deformation as a function of the energy spacing between the lowest $3/2^+$, $5/2^+$, $9/2^+$, and $11/2^-$ states, which becomes larger when the number of neutrons increases. A gradual spacing is also observed between the $15/2^-$ and $11/2^-$ states, the same as reported by Canchel *et al.* [77], which revealed that the deformation gradually increases when decreasing the neutron number.

However, from the systematics of the isotopic chain, our QPRM calculations showed that the systematic evolution of the band developed on the $1/2^+[420]$ intrinsic state could well be followed from the observed low-energy $5/2^+$ state. This result is furthermore consistent with the IBFM calculations as reported by Gizon [1] for ^{129}La , where a structure of spherical $g_{7/2}$ and $d_{5/2}$ orbitals was expected in the band built on the $5/2^+$ state. This state is, however, observed as the ground state for ^{123}La , which is not reproduced by our QPRM owing to the fact that the inertia parameter is adjusted for all studied bands. Furthermore, some discrepancies in describing the experimental data should be expected because we have limited our study to only γ -phonon excitation and neglected the other multipole modes of vibration (Q_{20} , β -phonon, $\beta\beta$ -phonon, $\gamma\gamma$ -phonon, etc.) and the multiphonon correlations which may be important in some nuclei from the transitional region [80].

IV. CONCLUSION

In summary, we presented an application of the quasiparticle-phonon coupling plus rotor approach (QPRM) to the transitional region of neighboring nuclei of ^{121}Cs , ^{125}Pr , and $^{123,125,127,129}\text{La}$. A detailed study of the low-energy level scheme of ^{123}La was made, by investigating how different terms of the Hamiltonian, such as the quadrupole, recoil,

and pairing interactions, influenced the position of the lowest intrinsic states and subsequently the rotational bands built upon them. The calculations showed that the low-energy structure bands are based either on one-quasiparticle states or on states with quasiparticle-phonon coupling terms. The contribution of the quasiparticle-phonon coupling plays a significant role in the configuration of the intrinsic states of both positive and negative parity. The calculations for ^{123}La predicted eight bands with bandheads situated at low energies, below 1000 keV, six of positive parity and two of negative parity. Three of the positive parity bands and one negative parity band were assigned to known experimental structures.

Based on these calculations, we have shown that the observed spectroscopic properties can be reasonably described as resulting from a competition between the quadrupole, recoil, and pairing forces. The quadrupole force tends to deform the nucleus (γ softness) in the situation where the pairing tends to stabilize a spherical shape. The pairing effect acting on a pair of quasiparticles combines the increasing rotation of the core with the Coriolis force acting in opposite ways on the pair of quasiparticles, resulting in an alignment of the angular momentum of each quasiparticle along the axis of rotation, which makes the quadrupole force active.

When more nucleons are added to a spherical shape nucleus (near a closed shell) the relative strength of the quadrupole force increases and leads, at a certain point, to the occurrence of deformed shape. We have studied these effects by extending the calculations to the isotonic chain of ^{121}Cs , ^{125}Pr and the isotopic chain of $^{125,127,129}\text{La}$ as well. The experimental ground state and the energy order of several excited states at low energies in these nuclei were reasonably well reproduced, excepting the observed lowest $5/2^+$ (ground) state of ^{123}La which we identified to belong to the $1/2^+[420]$ band. We showed, however, that the effect of deformation could be explained from the gradual evolution of energy spacing between low-energy ground states as a function of neutron number. We consequently learned that the positive parity states have configurations with important contributions from the quasiparticle-phonon coupling, while the negative parity states have large one-quasiparticle components where the Coriolis interaction is very pronounced for large angular momentum. In the concerned region, a strong mixture was shown between $\pi g_{7/2}$ and $\pi d_{5/2}$ orbitals which somehow makes it difficult to disentangle the potential low-energy states.

The study of the high spin behavior of the $1/2^-[550]$ bands in the transitional region of mass $A \approx 130$ requires a diagonalization of the total Hamiltonian for both rotational and deformed alignment. There, the rotational alignment favors states with negative parity, and the deformed one favors states with positive parity. Thus, a detailed reproduction of the observed level schemes in the particular transitional nuclear region considered in the present study is a challenge for this model. Nevertheless, the description obtained here for the low-energy level schemes in ^{121}Cs , ^{125}Pr , and $^{123,125,127,129}\text{La}$ can be considered a good step forward, towards a more detailed treatment, in progress now. New experimental information concerning firm spin and parity assignments and

absolute excitation energies of the low-energy states in these nuclei would be important for the calibration of these calculations.

Owing to the rarity of available data, we emphasize that for the studied La isotopes many of the low-energy states

have only tentative spin-parity assignments, and sometimes their positions relative to the ground state (absolute excitation energies) are not known. Therefore, the present calculations are also valuable for predicting possible solutions for these low-energy properties.

-
- [1] A. Gizon, J. Genevey, B. Weiss *et al.*, *Z Phys. A* **359**, 11 (1997).
- [2] A. Gizon, J. Genevey, D. Bucurescu, Gh. Căta-Danil, J. Gizon, J. Inchaouh, D. Barneoud, T. von Egidy, C. F. Liang, B. M. Nyakó, P. Paris, I. Penev, A. Plochocki, E. Ruchowska, C. A. Ur, B. Weiss, and L. Zolnai, *Nucl. Phys. A* **605**, 301 (1996).
- [3] J. Genevey, A. Gizon, D. Barnéoud *et al.*, *Z. Phys. A* **356**, 7 (1996).
- [4] A. Gizon, B. Weiss, P. Paris *et al.*, *Eur. Phys. J. A* **8**, 41 (2000).
- [5] K. Starosta, Ch. Droste, T. Morek, J. Srebrny, D. B. Fossan, S. Gundel, J. M. Sears, I. Thorslund, P. Vaska, M. P. Waring, S. G. Rohoziński, W. Sałata, U. Garg, S. Naguleswaran, and J. C. Walpe, *Phys. Rev. C* **55**, 2794 (1997).
- [6] R. Béraud, A. Emsallem, E. Chabanat *et al.*, *Acta Phys. Hung. New Ser.*, *Heavy Ion Phys.* **7**, 115 (1998).
- [7] M. Asai, Y. Kojima, A. Osa, M. Koizumi, T. Sekine, H. Yamamoto, and K. Kawade, Japan Atomic Energy Research Institute, Takasaki Ion Accelerator for Advanced Radiation Applications, Annual Report, 1993 (unpublished), p. 171 (1994).
- [8] J. Genevey, A. Gizon, N. Idrissi, B. Weiss, R. Béraud, A. Charvet, R. Duffait, A. Emsallem, M. Meyer, T. Ollivier, and N. Redon, in *Proceedings of the 5th International Conference on Nuclei Far from Stability, Rosseau Lake, Canada, 1987*, edited by I. S. Towner, AIP Conf. Proc. No. 164 (AIP, New York, 1988), p. 419.
- [9] D. D. Bogdanov, A. V. Demyanov, V. A. Karnaukhov, M. Nowick, L. A. Petrov, J. Vobořil, and A. Plochocki, *Nucl. Phys. A* **307**, 421 (1978).
- [10] Y. He and M. J. Godfrey, J. Jenkins, A. J. Kirwan, S. M. Mullins, P. J. Nolan, E. S. Paul, and R. Wadsworth, *J. Phys. G: Nucl. Part. Phys.* **18**, 99 (1992).
- [11] Y.-X. Xie, S.-W. Xu, Z.-K. Li, T.-M. Zhang, R.-C. Ma, Y.-X. Guo, Y.-X. Ge, C.-F. Wang, and J.-P. Xing, *High Energy Phys. Nucl. Phys. (China)* **25**, 198 (2001).
- [12] H. Iimura, M. Asai, S. Ichikawa, J. Katakura, M. Magara, A. Osa, M. Oshima, N. Shinohara, and H. Yamamoto, *Eur. Phys. J. A* **23**, 33 (2005).
- [13] C. M. Parry, R. Wadsworth, A. N. Wilson, A. J. Boston, P. J. Nolan, E. S. Paul, J. A. Sampson, A. T. Semple, C. Foin, J. Genevey, A. Gizon, J. Gizon, I. Ragnarsson, and B. G. Dong, *Phys. Rev. C* **61**, 021303(R) (2000).
- [14] A. N. Wilson, D. R. LaFosse, J. F. Smith, C. J. Chiara, A. J. Boston, M. P. Carpenter, H. J. Chantler, R. Charity, P. T. W. Choy, M. Devlin, A. M. Fletcher, D. B. Fossan, R. V. F. Janssens, D. G. Jenkins, N. S. Kelsall, F. G. Kondev, T. Koike, E. S. Paul, D. G. Sarantites, D. Seweryniak, K. Starosta, and R. Wadsworth, *Phys. Rev. C* **66**, 021305(R) (2002).
- [15] I. Sankowska, C. Droste, E. Grodner *et al.*, *Eur. Phys. J. A* **37**, 169 (2008).
- [16] M. Ionescu-Bujor, S. Aydin, A. Iordăchescu, N. Mărginean, S. Pascu, D. Bucurescu, C. Costache, N. Florea, T. Glodariu, A. Ionescu, R. Mărginean, C. Mihai, R. E. Mihai, A. Mitu, A. Negret, C. R. Niță, A. Olăcel, B. Saygi, L. Stroe, R. Suvăilă, S. Toma, and A. Turturică, *Phys. Rev. C* **102**, 044311 (2020).
- [17] D. J. Hartley, L. L. Riedinger, H. Q. Jin, W. Reviol, B. H. Smith, A. Galindo-Uribarri, D. G. Sarantites, D. R. LaFosse, J. N. Wilson, and S. M. Mullins, *Phys. Rev. C* **60**, 014308 (1999).
- [18] K. Starosta, Ch. Droste, T. Morek, J. Srebrny, D. B. Fossan, D. R. LaFosse, H. Schnare, I. Thorslund, P. Vaska, M. P. Waring, W. Sałata, S. G. Rohozinski, R. Wyss, I. M. Hibbert, R. Wadsworth, K. Hauschild, C. W. Beausang, S. A. Forbes, P. J. Nolan, and E. S. Paul, *Phys. Rev. C* **53**, 137 (1996).
- [19] S. Juutinen, P. Simecek, P. Ahonen, M. Carpenter, C. Fahlander, J. Gascon, R. Julin, A. Lampinen, T. Lonnroth, J. Nyberg, A. Pakkanen, M. Piiparinen, K. Schiffer, G. Sletten, S. Tormanen, and A. Virtanen, *Phys. Rev. C* **51**, 1699 (1995).
- [20] E. S. Paul, D. B. Fossan, Y. Liang, R. Ma, and N. Xu, *Phys. Rev. C* **40**, 1255 (1989).
- [21] E. S. Paul, C. W. Beausang, D. B. Fossan, R. Ma, W. F. Piel Jr, N. Xu, L. Hildingsson, and G. A. Leander, *Phys Rev Lett.* **58**, 984 (1987).
- [22] Y. S. Chen, S. Frauendorf, and G. A. Leander, *Phys. Rev. C* **28**, 2437 (1983).
- [23] J. Gizon, A. Gizon, R. M. Diamond, and F. S. Stephens, *Nucl. Phys. A* **290**, 272 (1977).
- [24] J. Gizon, A. Gizon, and J. Meyer-Ter-Vehn, *Nucl. Phys. A* **277**, 464 (1977).
- [25] J. Gizon and A. Gizon, *Z. Phys. A* **285**, 259 (1978).
- [26] A. V. Afanasjev and I. Ragnarsson, *Nucl. Phys. A* **608**, 176 (1996).
- [27] A. Galindo-Uribarri, D. Ward, H. R. Andrews, G. C. Ball, D. C. Radford, V. P. Janzen, S. M. Mullins, J. C. Waddington, A. V. Afanasjev, and I. Ragnarsson, *Phys. Rev. C* **54**, 1057 (1996).
- [28] H. I. Park, D. J. Hartley, L. L. Reidinger, W. Reviol, O. Zeidan, J. Y. Zhang, A. Galindo-Uribarri, R. V. F. Janssens, M. P. Carpenter, D. Seweryniak, D. G. Sarantites, M. Devlin, B. G. Dong, and I. Ragnarsson, *Phys. Rev. C* **68**, 044323 (2003).
- [29] J. Meyer-Ter-Vehn, *Nucl. Phys. A* **249**, 111 (1975).
- [30] S. E. Larsson, G. Leander, and I. Ragnarsson, *Nucl. Phys. A* **307**, 189 (1978).
- [31] F. Iachello and P. Van Isaker, *The Interacting Boson-Fermion Model* (Cambridge University Press, Cambridge, 1991).
- [32] Gh. Gata-Danil, D. Bucurescu, A. Gizon, and J. Gizon, *J. Phys. G* **20**, 1051 (1994).
- [33] R. Kuhn, I. Wiedenhöver, O. Vogel, L. Eßer, M. Wilhelm, A. Gelberg, and P. von Brentano, *Nucl. Phys. A* **594**, 87 (1995).
- [34] F. Lieden, B. Cederwall, P. Ahonen, D. W. Banes, B. Fant, J. Gascon, L. Hildingsson, A. Johnson, S. Juutinen, A. Kirwan, D. J. G. Love, S. Mitarai, J. Mukai, A. H. Nelson, J. Nyberg, J. Simpson, and R. Wyss, *Nucl. Phys. A* **550**, 365 (1992).
- [35] I. Ragnarsson and S. G. Nilsson, *Nucl. Phys. A* **158**, 155 (1970).

- [36] Y. Liang, R. Ma, E. S. Paul, N. Xu, D. B. Fossan, J.-Y. Zhang, and F. Dönau, *Phys. Rev. Lett.* **64**, 29 (1990).
- [37] V. G. Soloviev, *Theory of Complex Nuclei* (Pergamon Press, Oxford, 1976).
- [38] O. Jdair, Z. Housni, J. Inchaouh, A. Khouaja, M. Krim, H. Chakir, M. Fiak, M. Mouadil, Y. Elabssaoui, and M. Ferrichalami, *Nucl. Phys. A* **992**, 121639 (2019).
- [39] A. Boulal, J. Inchaouh, and M. K. Jammari, *Eur. Phys. J. A* **7**, 317 (2000).
- [40] J. Inchaouh, M. K. Jammari, O. Jdair, A. Khouaja, M. L. Bouhssa, H. Chakir, and A. Morsad, *Phys. Rev. C* **88**, 064301 (2013).
- [41] P. Möller, J. R. Nix, N. P. Mayer, and W. J. Swiatecki, *At. Data Nucl. Data Tables* **59**, 185 (1995).
- [42] S. G. Nilsson and I. Ragnarsson, in *Shapes and Shells in Nuclear Structure* (Cambridge University Press, Cambridge, 1995), p. 184.
- [43] J. Bardeen, L. N. Cooper, and J. R. Schrieffer, *Phys. Rev.* **106**, 162 (1957); **108**, 1175 (1957).
- [44] A. Bohr, B. R. Mottelson, and D. Pines, *Phys. Rev.* **110**, 936 (1958).
- [45] S. T. Belyaev, K. Dan Vidensk. Selsk. Mat. Fys. Medd. **31**, 11 (1959).
- [46] A. Bohr and B. R. Mottelson, *Nuclear Structure* (Benjamin, New York, 1975), Vol. 2.
- [47] P. Ring and P. Schuck, *The Nuclear Many-Body Problem* (Springer-Verlag, Berlin, 1980).
- [48] D. R. Bes and C. Yi-Chung, *Nucl. Phys.* **86**, 581 (1966).
- [49] J. M. Eisenberg and W. Greiner, *Nuclear Models* (Elsevier, New York, 1970), Vol. 1.
- [50] J. P. Boisson and R. Piepenbring, *Nucl. Phys. A* **168**, 385 (1971).
- [51] P. Möller and J. R. Nix, *Nucl. Phys. A* **536**, 20 (1992).
- [52] N. Idrissi, A. Gizon, J. Genevey, P. Paris, V. Barci, D. Barneoud, J. Blachot, D. Bucurescu, R. Duffait, J. Gizon, C. F. Liang, and B. Weiss, *Z. Phys. A* **341**, 427 (1992).
- [53] Y. Kojima, M. Asai, M. Shibata, K. Kawade, A. Taniguchi, A. Osa, M. Koizumi, and T. Sekine, *Appl. Radiat. Isot.* **56**, 543 (2002).
- [54] K. Kitao, Y. Tendow, and A. Hashizume, *Nucl. Data Sheets* **96**, 241 (2002).
- [55] T. Tamura, *Nucl. Data Sheets* **108**, 455 (2007).
- [56] J. Katakura and K. Kitao, *Nucl. Data Sheets* **97**, 765 (2002).
- [57] J. Katakura and Z. D. Wu, *Nucl. Data Sheets* **109**, 1655 (2008).
- [58] L. Grodzins *et al.*, *Phys. Lett.* **2**, 88 (1962).
- [59] F. S. Stephens, R. M. Diamond, J. R. Leigh, T. Kammuri, and K. Nakai, *Phys. Rev. Lett.* **29**, 438 (1972).
- [60] C. M. Petrache, Y. Sun, D. Bazzacco, S. Lunardi, C. Rossi Alvarez, R. Venturelli, D. De Acuña, G. Maron, M. N. Rao, Z. Podolyák, and J. R. B. Oliveira, *Phys. Rev. C* **53**, R2581(R) (1996).
- [61] J. Y. Zhang, N. Xu, D. B. Fossan, Y. Liang, R. Ma, and E. S. Paul, *Phys. Rev. C* **39**, 714 (1989).
- [62] T. Bengtsson and I. Ragnarsson, *Nucl. Phys. A* **436**, 14 (1985).
- [63] <http://www.nndc.bnl.gov/nudat2/getdataset.jsp?nucleus=141NDunc=nds>
- [64] R. Wyss, A. Grandenath, R. Bengtsson, P. von Brentano, A. Dewald, A. Gelberg, A. Gizon, J. Gizon, S. Harissopulos, A. Johnson, W. Lieberz, W. Nazarewicz, J. Nyberg, and K. Schiffer, *Nucl. Phys. A* **505**, 337 (1989).
- [65] Z. Sheng-Jiang, M. Sakhaee, Y. Li-Ming, G. Cui-Yun, Z. Ling-Yan, X. Rui-Qing *et al.*, *Chin. Phys. Lett.* **18**, 1027 (2001).
- [66] C. Petrache, G. Lo Bianco, D. Bazzacco *et al.*, *Eur. Phys. J. A* **12**, 135 (2001).
- [67] C. Fransen, N. Pietralla, A. Linnemann, V. Werner, and R. Bijker, *Phys. Rev. C* **69**, 014313 (2004).
- [68] R. F. Casten and P. Von Brentano, *Phys. Lett. B* **152**, 22 (1985).
- [69] R. Wyss, F. Lidén, J. Nyberg, A. Johnson, D. J. G. Love, A. H. Nelson, D. W. Banes, J. Simpson, A. Kirwan, and R. Bengtsson, *Nucl. Phys. A* **503**, 244 (1989).
- [70] K. E. G. Löbner, in *The Electromagnetic Interaction in Nuclear Spectroscopy*, edited by W. D. Hamilton (North-Holland, Oxford, 1975), p. 141.
- [71] S. Ohya, *Nucl. Data Sheets* **102**, 547 (2004).
- [72] R. M. Lieder and H. Ryde, in *Advances in Nuclear Physics*, edited by M. Baranger and E. Vogt (Plenum, New York, 1978), p. 1.
- [73] *Handbook of Nuclear Chemistry, Vol. 1: Basics of Nuclear Science*, 2nd ed., edited by A. Vértes, S. Nagy, Z. Klencsar, R. G. Lovas, and F. Rosch (Springer-Verlag, Berlin, 2010), p. 96.
- [74] S. Ohya, *Nucl. Data Sheets* **111**, 1619 (2010).
- [75] J. Katakura, *Nucl. Data Sheets* **112**, 495 (2011).
- [76] P. D. Cottle, T. Glasmacher, and K. W. Kemper, *Phys. Rev. C* **45**, 2733 (1992).
- [77] G. Canchel, R. Béraud, E. Chabanat, A. Emsallem, N. Redon, P. Dendooven, J. Huikari, A. Jokinen, V. Kolhinen, G. Lhersonneau *et al.*, *Eur. Phys. J. A* **5**, 1 (1999).
- [78] A. Hashizume, *Nucl. Data Sheets* **112**, 1647 (2011).
- [79] J. Timar, Z. Elekes, and B. Singh, *Nucl. Data Sheets* **121**, 143 (2014).
- [80] M. K. Jammari and R. Piepenbring, *Nucl. Phys. A* **487**, 77 (1988).